Progress In Electromagnetics Research, Vol. 141, 219–231, 2013

DUAL-BAND POLARIZATION INDEPENDENT METAMATERIAL ABSORBER BASED ON OMEGA RESOANATOR AND OCTA-STARSTRIP CONFIGURATION

Furkan Dincer[1], Muharrem Karaaslan[1], Emin Unal[1], and Cumali Sabah[2, *]

[1]Department of Electrical and Electronics Engineering, Mustafa Kemal University, Iskenderun, Hatay 31200, Turkey

[2]Department of Electrical and Electronics Engineering, Middle East Technical University, Northern Cyprus Campus, Kalkanli, Guzelyurt, TRNC/Mersin 10, Turkey

Abstract—Dual-band metamaterial absorber (MA) with polarization independency based on omega (Ω) resonator with gap and octa-star strip (OSS) configuration is presented both numerically and experimentally. The suggested MA has a simple configuration which introduces flexibility to adjust its metamaterial (MTM) properties and easily re-scale the structure for other frequencies. In addition, the dual-band character of the absorber provides additional degree of freedom to control the absorption band(s). Two maxima in the absorption are experimentally obtained around 99% at 4.0 GHz for the first band and 79% at 5.6 GHz for the second band which are in good agreement with the numerical simulations (99% and 84%, respectively). Besides, numerical simulations validate that the MA could achieve very high absorption at wide angles of incidence for both transverse electric (TE) and transverse magnetic (TM) waves. The proposed MA and its variations enable myriad potential applications in medical technologies, sensors, modulators, wireless communication, and so on.

1. INTRODUCTION

MTMs have gained considerable attention [1–10] due to their unusual features and beneficial applications in numerous devices for different regimes of EM spectrum [11–15]. The concept was started by Veselago in 1968 [16] and continued with the studies of Pendry

Received 11 June 2013, Accepted 9 July 2013, Scheduled 13 July 2013

* Corresponding author: Cumali Sabah (sabah@metu.edu.tr).

and his colleagues [17]. After that, the first experimental study on MTMs at microwave frequencies was performed by Smith and Kroll in 2000 [18]. Since then, MTM topology continues to be of great interest and practical importance owing to a variety of potential applications due to the common/special needs in science and technology [19–36]. In this sense, many research groups have studied the EM response of MTMs in order to understand their fundamental features and investigated their variations to be used in many applications such as lenses, antennas, sensors, absorbers, and so on. With this regard, the motivation of this study is to design, realize, and analyze a perfect MTM absorber to be used in appropriate applications. Bilotti et al. in 2007 studied the absorber concept based on MTM structure and show that MTMs can be used to enhance the efficiency of the absorber based devices [19]. After that, studies on MTM absorber have attracted significant attention by many researchers during the last five years due to the potential advantages of low cost processes, mechanical flexibility, and fabrication simplicities [20–25].

In this study, a new dual-band MTM absorber composed of Ω resonator with gap and OSS configuration for microwave region is suggested and investigated both numerically and experimentally. The novel design has simple geometrical pattern which allows the simplification in the manufacturing process and provides dual absorption bands as well as the rescaling (scale-up and down) in the structure for different frequencies. The structure shows a strong resonance and provides perfect absorption at 4.0 GHz which is validated by both simulation and experimental studies. The surface current and electric field distributions are also analyzed to demonstrate and verify the physical mechanism of the absorber. Consequently, the proposed structure with high quality features will be a good candidate among its counterparts and can be used in many MTM applications.

2. DESIGN, SIMULATION, AND EXPERIMENT

As mentioned before, the proposed design consist Ω resonator with gap as an external pattern and OSS configuration as internal patterns in the unit cell which shown in Figure 1. The metallic structures on the top and bottom layers of the substrate are chosen as copper with the electrical conductivity of 5.8×10^7 S/m and thickness of 0.036 mm. FR4 is selected as a substrate with the thickness of 1.6 mm. The thickness, loss tangent, and relative permittivity of the substrate are 1.6 mm, 0.02, and 4.2, respectively. The dimensions of the structure are presented in Figure 1(a). After the design, the sample is fabricated with the overall size of 225 cm^2 (5×5 unit cells) which is shown in Figure 1(b). The

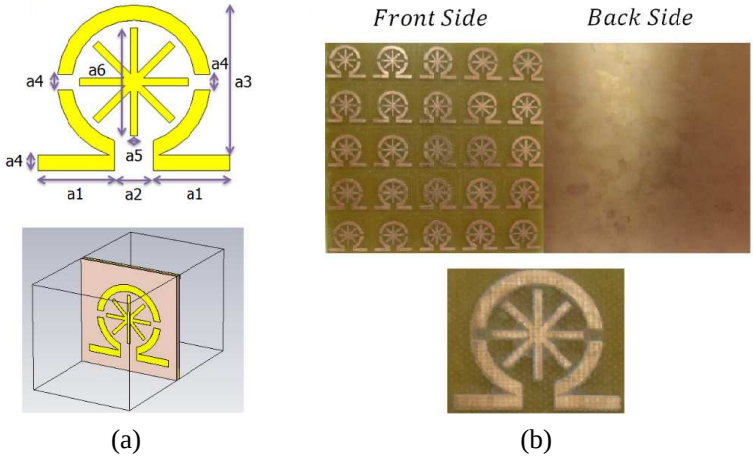

Figure 1. Designed and fabricated absorber. (a) Unit cell with dimensions. (b) Picture of the sample.

dimensions are $a1 = 10\,\text{mm}$, $a2 = 5\,\text{mm}$, $a3 = 20\,\text{mm}$, $a4 = 2\,\text{mm}$, $a5 = 1\,\text{mm}$, and $a6 = 14\,\text{mm}$.

The simulation of the periodic structure was performed with a commercial full-wave EM solver based on finite integration technique. The periodic boundary conditions with floquet port is used in the simulation. The measurement is carried out by using R&S ZVL6 Vector Network Analyzer (VNA) and two horn antennas. In the measurement, one horn acts as a transmitter and the other one detects the transmitted or reflected wave. Firstly, free space measurement without sample is carried out and this measurement used as the calibration data for the VNA. The sample is then inserted into the

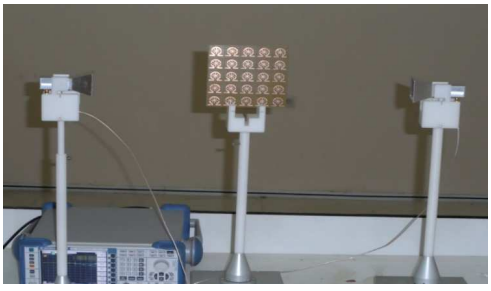

Figure 2. A picture from the experiment.

experimental measurement setup and S-parameters measurements are performed. The sample and devices used in the measurement are shown in Figure 2. Note that the transmitter antenna and the front side of the sample are arranged to form face-to-face configuration with each other in the measurement.

3. NUMERICAL AND EXPERIMENT RESULTS

First of all, the numerical study is performed for the MTM absorber structure. After that, the results are verified by measuring the S-parameters. As known, the proposed structure will not have transmission because of the metallic plate located at its back side. The selected geometry provides strong absorption at a certain frequency because of structural properties which minimizes the reflection for the applied incident EM wave and can suitably be used in many applications where perfect absorption is required. In addition, there is a second absorption band in which the reflection is also minimum. The frequency characteristic of absorption can be calculated by $A(\omega) = 1-R(\omega)-T(\omega)$. The idea of maximizing absorption, $A(\omega)$, comes from minimizing both the reflection $R(\omega) = |S_{11}|^2$ and transmission $T(\omega) = |S_{21}|^2$ at the resonance frequency. There will be no transmission to be examined throughout the present study as mentioned before, as it is blocked off by the continuous metal. Therefore, only the reflection needs to be investigated which is directly related with S_{11}. Consequently, the absorption can be calculated as $A(\omega) = 1 - R(\omega)$. The absorption may achieve unity when the reflection is close to zero which is the main aim of the study.

Figures 3 and 4 show the simulation and measurement results

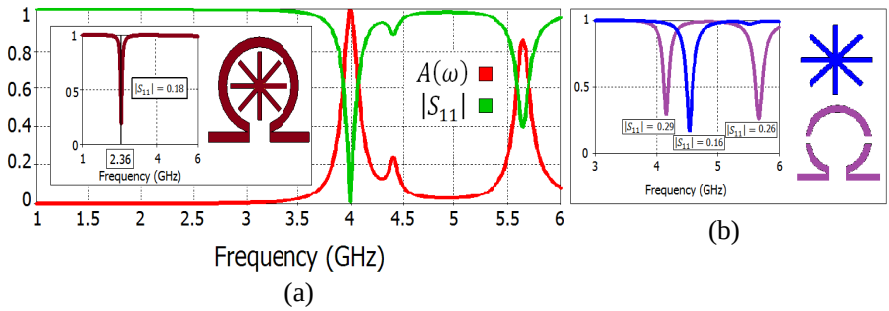

Figure 3. (a) Simulated reflection and absorption for the proposed microwave absorber. Inset: reflection spectrum of the MTM absorber with no gap in the Ω resonator. (b) Reflection performances of Ω resonator and OSS structure individually.

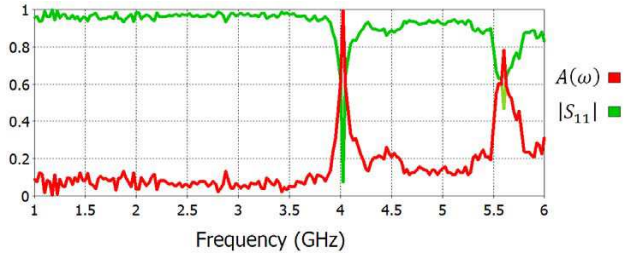

Figure 4. Measured reflection and absorption for the proposed microwave absorber.

for the reflection and absorption spectra. Two different resonances occur around 4.0 GHz and 5.6 GHz in the reflection spectrum, thus yielding two maxima in the absorption. The first peak is about 99% both in the simulation and experiment and the second one is 84% in the simulation and 79% in the experiment. The simulation results are in good agreement with the experimental ones. The inset of Figure 3 shows the reflection response of the structure without gap in the Ω resonator. As seen, the reflection has only one resonance with the magnitude of 0.18 at 2.36 GHz in this case. This means that the gaps in the Ω resonator make the reflection smaller and provide the second absorption band. The shift in the resonance for the structure without gap with respect to the original one can be explained by the change of the capacitance and inductance values. Moreover, for the first resonance, the reflection is very close to zero which means the effective impedance $Z(\omega) = \sqrt{\mu(\omega)/\varepsilon(\omega)}$ of the medium matches with the free space impedance $Z(\omega) = Z_0(\omega) = 120\pi$, and therefore, the reflection is minimized [24–27]. This concept is proved both numerically and experimentally in which the sample has zero reflection at the resonance. For the second band, perfect impedance matching is not fulfilled. Thus, the structure provides two distinct absorption bands in which the first one is perfect and the second one is relatively good. Therefore, the proposed model can be a good practical candidate among its counterparts operated at the same frequency region reported in literature. Furthermore, the bandwidth calculations are also performed to show quality of the proposed absorber. So that, the fractional bandwidth (FBW) of the absorption region is calculated. FBW can be found by dividing the bandwidth of the absorber to its center frequency. It can be calculated as $FBW = \Delta f/f_0$, where Δf is the half power bandwidth and f_0 is the center frequency. For the first resonance, these parameters are calculated as $\Delta f = 0.19$ GHz, $f_0 = 4.0$ GHz and $FBW \approx 4.76\%$ from the simulation and $\Delta f = 0.25$,

$f_0 = 4.02\,\text{GHz}$, and $FBW \approx 6.21\%$ for the experiment. For the second resonance, the related parameters are $\Delta f = 0.182$, $f_0 = 5.64\,\text{GHz}$, and $FBW \approx 3.23\%$ from the simulation and $\Delta f = 0.31$, $f_0 = 5.6\,\text{GHz}$, and $FBW \approx 5.53\%$ from the experiment. These computations signify that the proposed structure has good quality character [34–36]. Moreover, reflection (correspondingly absorption) performances of Ω resonator and OSS structure separately are shown in the right side of Figure 3. As seen from the figure, single and double resonances are observed for the OSS structure and Ω resonator, respectively. The performances of the individual elements are not perfect for the main resonance as in the combined one. This means that the combination of the individual elements operates effectively together and provides perfect absorption for the main mode. However, the performance of the second mode in the individual structure for Ω resonator with gap is better than the combined structure. Note that, the absorption for the second mode for the combined structure is around 80% in which it can be accepted as the second absorption band. Note again, the reflection (absorption) spectra for both individual elements between 1.0 GHz and 3.0 GHz are unity (zero) which is not shown in the figure.

In order to better understand the physical mechanism of the operation principle of the structure at the resonances, the electric field and surface current distributions are investigated at the resonant frequency of 4.0 GHz. The results are shown in Figures 5 and 6. High concentration of the electric field around the corner of OSS, the tails of Ω resonator, and the gap, in order, is observed. The electric field are strongly coupled with the strips and supply independent electric response as working like a dipole for all polarizations. As a result, the surface charges oscillate along the external electric field. Consequently, a magnetic dipole is excited, induces a magnetic response, and causes a resonant absorption. It was observed that there is circulating, parallel, and anti-parallel currents in the pattern. The circulating and anti-parallel currents are responsible from the magnetic response while the parallel currents are in charge for the electric response. Thus, the mentioned currents are driven by strong magnetic and/or electric coupling. They induces magnetic and electric responses which can strongly couple with the corresponding field of the incident EM wave. Therefore, strong localized EM field enhancement is established at the resonance frequency. It indicates that electric and magnetic resonances appear at this resonant frequency simultaneously, which provide the ability to absorb the EM radiation almost completely under the matching condition ($Z(\omega) = Z_0(\omega)$). Thus, EM energy is confined in the structure, which yields near zero reflection and unity absorption. Furthermore, similar observations are also monitored for

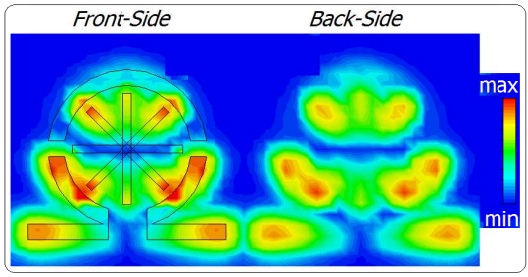

Figure 5. Electric field distribution at the resonant frequency of 4.0 GHz for the front and back side of the unit cell.

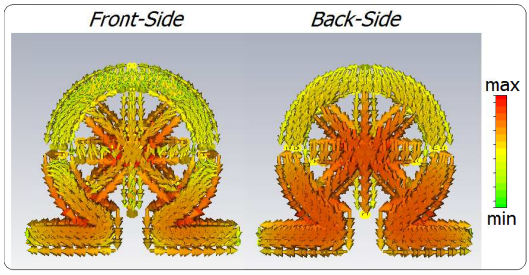

Figure 6. Surface current distribution at resonance frequency of 4.0 GHz for the front and back side of the unit cell.

the other resonance located at 5.6 GHz expect its mode as shown in Figures 7 and 8. Electric filed is concentrated at the upper side of the Ω resonator as seen in the figure. The same current distribution is also observed. This means that electric and magnetic resonances appear at this resonant frequency too as before. However, this mode is not stronger as in the previous one thus yielding reasonable absorption compared to the previous one. Note that it averagely provides 80% absorption although it is relatively weaker than first resonance.

In the second exploration, the effects of the incidence angle on the behavior of the absorber is examined. Figure 9 shows the frequency response of the reflection and absorption for the mentioned process. It can be seen that the proposed absorber provides very well absorption for all incident angles. Especially, for the first resonance (4.0 GHz), the variation in the absorption with respect to frequency is very small and the absorption peak is still around 99%. This peak is also tested experimentally which can be seen from right panel of Figure 9. It continues to provide the same feature for all angles at the first

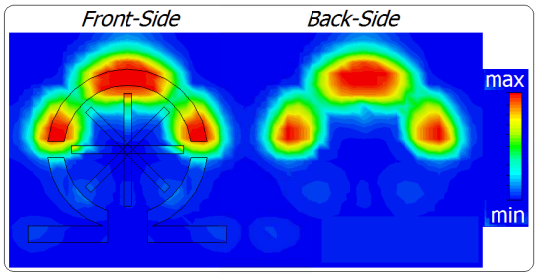

Figure 7. Electric field distribution at the resonant frequency of 5.6 GHz for the front and back side of the unit cell.

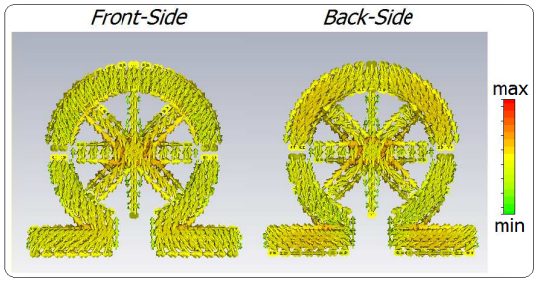

Figure 8. Surface current distribution at resonance frequency of 5.6 GHz for the front and back side of the unit cell.

resonance with very small shift (less than 1%) even the incident angle is 90° off normal. The second peak has decreasing and increasing features depending on the angle of incident. The additional peaks occur in the spectra can be explained with the phenomenon of oblique incidence. In this case, additional part of the reflected wave can also be transformed because of non-zero components of the perpendicular and/or parallel components of the incident EM wave, as seen from the figures.

As the next investigation, the effect of the polarization on the frequency response of the absorber is analyzed. The simulated absorption characteristics as a function of the frequency for the transverse electric (TE) and transverse magnetic (TM) polarized EM waves for different polarization angles are obtained by simulation and the results are shown in Figure 10. It is seen that the main peak of the absorption is around unity again (∼99%) for the TE and TM cases at the normal incidence. A unity absorption is preserved for the TM case while it is decreased for the TE case (still around and/or above 90%) when the incident angle changes at the main

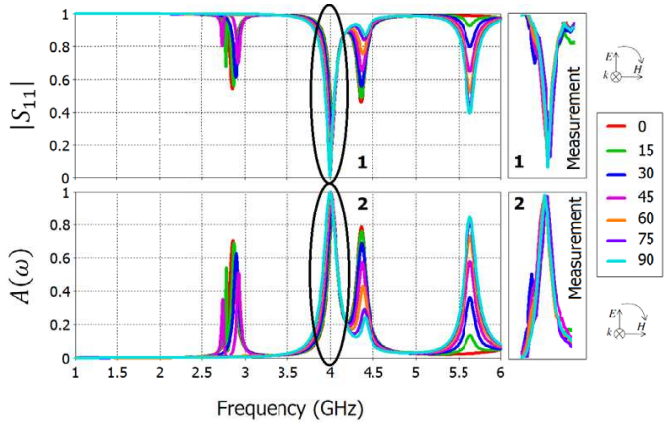

Figure 9. Simulated results of the absorbing performance under different polarization angles for the case of normal incidence.

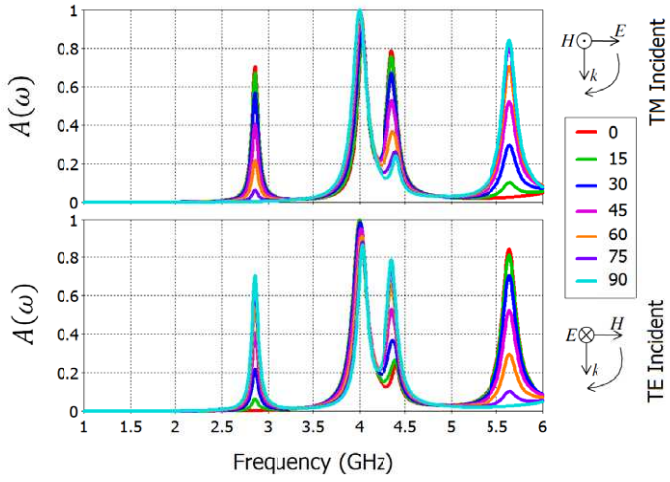

Figure 10. Simulated results of the absorbing performance under different polarization angles for TE and TM polarizations.

resonance. The shift in the resonance frequency is still very small as in the previous cases. The second as well as the additional peaks increased or decreased depending on polarization and the incident angle. The results show that the absorber has almost no polarization dependency for the main peak for the any arbitrary polarization with wide range of incident angles. The magnitude of the other peaks varies depending on the type of the polarization and indecent angle as

mentioned. Consequently, the proposed design can be used as a perfect absorber with the availability of wide-angle incidence and polarization independency, which is very useful for the medical applications such as medical imaging, since different polarizations and different angles provide nearly same absorption character.

4. CONCLUSION

The absorption properties of MTM absorber composed of Ω resonator and cross-wire-strips are studied and discussed based on the experimental and simulation results. The proposed absorber has simple geometry and shows very efficient results for the studied microwave range. The experimental results are in good agreement with the numerical simulations. The simulated measured resonant absorption with close to unity magnitude ($\sim 99\%$) appeared at 3.99 GHz. The bandwidth and quality factor of the absorber are relatively good with respect to its counterparts. This means that the performance of the structure is quite good for the microwave region. In addition, the structure is also analyzed when the incident angle and polarization state of the EM incident is changed. It shows very good performance for the mentioned variations and the absorption is kept around unity ($\sim 99\%$) almost for all changes. Furthermore, the electric field and surface current distributions are presented and analyzed to understand the resonance absorption mechanism. As a result, the proposed absorber can serve as a model guide to design new absorbers for higher frequencies and can be used in many applications such as medical imaging, sensors, wireless communications.

ACKNOWLEDGMENT

The assistance of M. Bakir is acknowledged with respect to the preparation of the sample.

REFERENCES

1. Huang, L. and H. Chen, "Multi-band and polarization insensitive metamaterial absorber," *Progress In Electromagnetics Research*, Vol. 113, 103–110, 2011.
2. Sabah, C., H. T. Tastan, F. Dincer, K. Delihacioglu, M. Karaaslan, and E. Unal, "Transmission tunneling through the multi-layer double-negative and double-positive slabs," *Progress In Electromagnetics Research*, Vol. 138, 293–306, 2013.

3. Sabah, C. and H. G. Roskos, "Design of a terahertz polarization rotator based on a periodic sequence of chiral metamaterial and dielectric slabs," *Progress In Electromagnetics Research*, Vol. 124, 301–314, 2012.
4. Dincer, F., C. Sabah, M. Karaaslan, E. Unal, M. Bakir, and U. Erdiven, "Asymmetric transmission of linearly polarized waves and dynamically wave rotation using chiral metamaterial," *Progress In Electromagnetics Research*, Vol. 140, 227–239, 2013.
5. Cheng, Y., Y. Nie, L. Wu, and R. Gong, "Giant circular dichroism and negative refractive index of chiral metamaterial based on split-ring resonators," *Progress In Electromagnetics Research*, Vol. 138, 421–432, 2013.
6. Boyvat, M. and C. Hafner, "Magnetic field shielding by metamaterials," *Progress In Electromagnetics Research*, Vol. 136, 647–664, 2013.
7. He, Y., J. Shen, and S. He, "Consistent formalism for the momentum of electromagnetic waves in lossless dispersive metamaterials and the conservation of momentum," *Progress In Electromagnetics Research*, Vol. 116, 81–106, 2011.
8. Hasar, U. C., J. J. Barroso, M. Ertugrul, C. Sabah, and B. Cavusoglu, "Application of a useful uncertainty analysis as a metric tool for assessing the performance of electromagnetic properties retrieval methods of bianisotropic metamaterials," *Progress In Electromagnetics Research*, Vol. 128, 365–380, 2012.
9. Sabah, C. and S. Uckun, "Multilayer system of lorentz/drude type metamaterials with dielectric slabs and its application to electromagnetic filters," *Progress In Electromagnetics Research*, Vol. 91, 349–364, 2009.
10. Sabah, C., "Multiband metamaterials based on multiple concentric open-ring resonators topology," *IEEE Journal of Selected Topics in Quantum Electronics*, Vol. 19, 8500808, 2013.
11. Smith, D. R., W. J. Padilla, D. C. Vier, S. C. Nemat-Nasser, and S. Schultz, "Composite medium with simultaneously negative permeability and permittivity," *Phys. Rev. Lett.*, Vol. 84, 4184–4187, 2000.
12. Yen, T. J., W. J. Padilla, N. Fang, D. C. Vier, D. R. Smith, J. B. Pendry, D. N. Basov, and X. Zhang, "Terahertz magnetic response from artificial materials," *Science*, Vol. 303, 1494–1496, 2004.
13. Linden, S., C. Enkrich, M. Wegener, J. Zhou, T. Koschny, and C. M. Soukoulis, "Magnetic response of metamaterials at 100 Terahertz," *Science*, Vol. 306, 1351–1353, 2004.

14. Zhang, S., W. Fan, N. C. Panoiu, K. J. Malloy, R. M. Osgood, and S. R. J. Brueck, "Experimental demonstration of near-infrared negative-index metamaterials," *Phys. Rev. Lett.*, Vol. 95, 137404-4, 2005.
15. Dolling, G., M. Wegener, C. M. Soukoulis, and S. Linden, "Negative-index metamaterial at 780 nm wavelength," *Opt. Lett.*, Vol. 32, 53–55, 2007.
16. Veselago, V. G., "The electrodynamics of substances with simultaneously negative values of ε and μ," *Physics Uspekhi*, Vol. 10, 509–514, 1968.
17. Pendry, J. B., A. J. Holden, W. J. Stewart, and I. Youngs, "Extremely low frequency plasmons in metallic mesostructures," *Phys. Rev. Lett.*, Vol. 76, 4773–4776, 1996.
18. Smith, D. R. and N. Kroll, "Negative refraction index in left-handed materials," *Phys. Rev. Lett.*, Vol. 85. 2933–2936, 2000.
19. Bilotti, F., L. Nucci, and L. Vegni, "An SRR-based microwave absorber," *Microwave and Optical Technology Letters*, Vol. 48, 2171–2175, 2006.
20. Landy, N. I., S. Sajuyigbe, J. J. Mock, D. R. Smith, and W. J. Padilla, "A perfect metamaterial absorber," *Phys. Rev. Lett.*, Vol. 100, 207402-4, 2008.
21. Wang, B., T. Koschny, and C. M. Soukoulis, "Wide-angle and polarization-independent chiral metamaterial absorber," *Physical Review B*, Vol. 80, 033108-4, 2009.
22. Zhu, B., Z. Wang, C. Huang, Y. Feng, J. Zhao, and T. Jiang, "Polarization insensitive metamaterial absorber with wide incident angle," *Progress In Electromagnetics Research*, Vol. 101, 231–239, 2010.
23. Zhu, B., Y. Feng, J. Zhao, C. Huang, Z. Wang, and T. Jiang, "Polarization modulation by tunable electromagnetic metamaterial reflector/absorber," *Optics Express*, Vol. 18, 23196–23203, 2010.
24. Lee, J. and S. Lim, "Bandwidth-enhanced and polarization-insensitive metamaterial absorber using double resonance," *Electronics Letters*, Vol. 47, 8–9, 2011.
25. Huang, Y. J., G. J. Wen, J. Li, W. R. Zhu, P. Wang, and Y. H. Sun, "Wide-angle and polarization independent metamaterial absorber based on snowflake-shaped configuration," *Journal of Electromagnetic Waves and Applications*, Vol. 27, No. 5, 552–559, 2013.
26. Li, M. H., H. L. Yang, and X. W. Hou, "Perfect metamaterial

absorber with dual bands," *Progress In Electromagnetics Research*, Vol. 108, 37–49, 2010.

27. He, X. J., Y. Wang, J. M. Wang, and T. L. Gui, "Dual-band terahertz metamaterial absorber with polarization insensitivity and wide incident angle," *Progress In Electromagnetics Research*, Vol. 115, 381–397, 2011.
28. Wang, B. and K. M. Huang, "Spatial microwave power combining with anisotropic metamaterials," *Progress In Electromagnetics Research*, Vol. 114, 195–210, 2011.
29. Butt, H., Q. Dai, T. D. Wilkinson, and G. A. J. Amaratunga, "Photonic crystals & metamaterial filters based on 2D arrays of silicon nanopillars," *Progress In Electromagnetics Research*, Vol. 113, 179–194, 2011.
30. Cojocaru, E., "Electromagnetic tunneling in lossless trilayer stacks containing single-negative metamaterials," *Progress In Electromagnetics Research*, Vol. 113, 227–249, 2011.
31. Gric, T., L. Nickelson, and S. Asmontas, "Electrodynamical characteristic particularity of open metamaterial square and circular waveguides," *Progress In Electromagnetics Research*, Vol. 109, 361–379, 2010.
32. Choi, J. and C. H. Seo, "High-efficiency wireless energy transmission using magnetic resonance based on negative refractive index metamaterial," *Progress In Electromagnetics Research*, Vol. 106, 33–47, 2010.
33. Ourir, A., R. Abdeddaim, and J. de Rosny, "Tunable trapped mode in symmetric resonator designed for metamaterials," *Progress In Electromagnetics Research*, Vol. 101, 115–123, 2010.
34. Yilmaz, A. and C. Sabah, "Diamond-shaped hole array in double-layer metal sheets for negative index of refraction," *Journal of Electromagnetic Waves and Applications*, Vol. 27, No. 4, 413–420, 2013.
35. Alici, K. B. and E. Ozbay, "Theoretical study and experimental realization of a low-loss metamaterial operating at the millimeter-wave regime: Demonstrations of flat- and prism-shaped samples," *IEEE Journal of Selected Topics in Quantum Electronics*, Vol. 16, 386–393, 2010.
36. Ziolkowski, R. W., "Metamaterial-based source and scattering enhancements: From microwave to optical frequencies," *Opto-Electronics Review*, Vol. 14, 167–177, 2006.